

# Design of Probe-Fed Stacked Patches

Rod B. Waterhouse, *Member, IEEE*

**Abstract**—In this paper, a design strategy to achieve bandwidths in excess of 25% for probe-fed stacked patches is presented. The choice of appropriate dielectric materials for such bandwidths is given and the role of each antenna parameter in controlling the impedance behavior is provided. It has been found that the selection of the substrate below the lower patch plays a major role in producing broad-band responses. A simple design procedure is outlined and this technique is verified experimentally. The findings presented here can be applied to all types of probe-fed stacked patches as well as edge-fed and cavity-backed configurations.

**Index Terms**—Printed antennas.

## I. INTRODUCTION

PROBE-FED microstrip patches have re-emerged as a popular candidate for a variety of antenna systems due to their robust nature. As a result of the direct contact between the probe and the patch radiator, these printed antennas minimize dielectric layer misalignment difficulties that can be encountered when say aperture-coupled patches are used at very high frequencies. Probe-fed microstrip antennas also provide excellent isolation between the feed network and the radiating elements and yield very good front-to-back ratios. These latter points are very important for applications where multiple arrays are located back-to-back in close proximity such as for mobile base station antennas or local multipoint distribution systems (LMDS) antennas.

A fundamental limit of the probe-fed patch antenna has been the achievable impedance bandwidth. Here, 10-dB return-loss bandwidths approaching 8% have been obtained for a single-element configuration if foam is used as the substrate [1], however, this is by no means adequate for most wireless systems. Parasitically coupling another printed antenna to the driven patch—or stacking—has alleviated this problem to a degree, however, probe-fed configurations with bandwidths of less than 15% have typically only been achieved. Once again, this is not enough for most communication links, allowing for the degree of error caused by dielectric constant and thickness variations in the required material. It was postulated that this bandwidth barrier was due to the inductive nature of the feed and so impedance control of the radiator when thick substrates were used was very difficult. Thus, several methods have been proposed to overcome this inherent difficulty including offsetting the coupled patch or modifying the feed contact (for example, [2]). Although these techniques circumvent the problem to an extent, they undermine the inherent advantages

of the probe-fed configuration, namely its robustness and its reduction in alignment errors.

An accurate computationally fast analysis is an important building block for the design of printed antennas with enhanced performance. Recently, bandwidths approaching an octave were achieved for an aperture-stacked patch antenna configuration [3], however, without the utilization of a full wave analysis, it could be argued that such extreme bandwidths would not have been obtained due to the electromagnetic complexity of the radiating structure. Several researchers have developed accurate analyzes for a probe-fed patch microstrip patch antenna [4]–[6]. In [7], the attachment mode developed by Aberle and Pozar [4] was utilized in a probe-fed stacked-patch configuration, yielding an antenna with a bandwidth approaching 25%, once again highlighting the significance of an accurate fast analysis tool. This order of bandwidth is compliant with most wireless systems, however, unfortunately a design procedure was not given in [7] for the development of these broad-band probe-fed patches.

In this paper, design trends for broad-band probe-fed stacked patches are established. Here broad-band is defined as a 10-dB return-loss bandwidth greater than 25%. In a similar vain to [3], the objective of this work is to develop a robust design philosophy for stacked-patch designs including how to start the design procedure and which dimensions of the printed antenna should be varied to achieve the desired impedance response. The characteristics and impedance trends of probe-fed stacked circular, rectangular, and annular rings will be presented. It will be shown that all three configurations behave effectively in the same manner and varying one parameter on say the circular patch geometry has the same effect when changing a similar parameter on the other geometries. It will be shown that annular rings and rectangular stacked patches do offer an extra degree of freedom compared to circular patches. This gives easier impedance control at the expense of slightly reduced bandwidth.

## II. GEOMETRIES, THEORY AND VALIDATION

Fig. 1 shows cross-sectional views of the considered probe-fed stacked circular, rectangular, and annular ring patches. As can be seen from this figure, the bottom patch of each configuration is fed by a coaxial feed through the ground plane. To accurately analysis each probe-fed stacked-patch arrangement rigorous, full wave analyses were devised based on the spectral-domain integral-equation approach (refer to [4], [8], and [9] for details of the formulation). It should be noted that the formulation for each geometry accurately models the discontinuity associated with the probe-patch interconnect. The

Manuscript received October 21, 1998; revised August 26, 1999.

The author is with the Department of Communication and Electronic Engineering, RMIT University, Melbourne, VIC 3001 Australia.

Publisher Item Identifier S 0018-926X(99)09979-2.

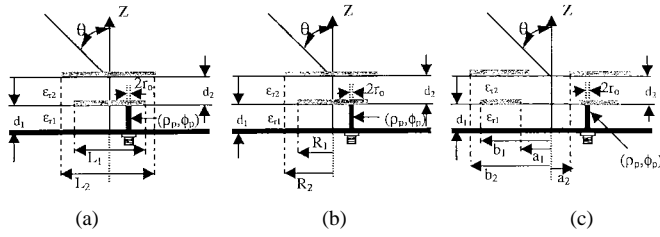


Fig. 1. Cross-sectional views of probe-fed stacked-patch geometries. (a) Rectangular patches. (b) Circular patches. (c) Annular ring patches.

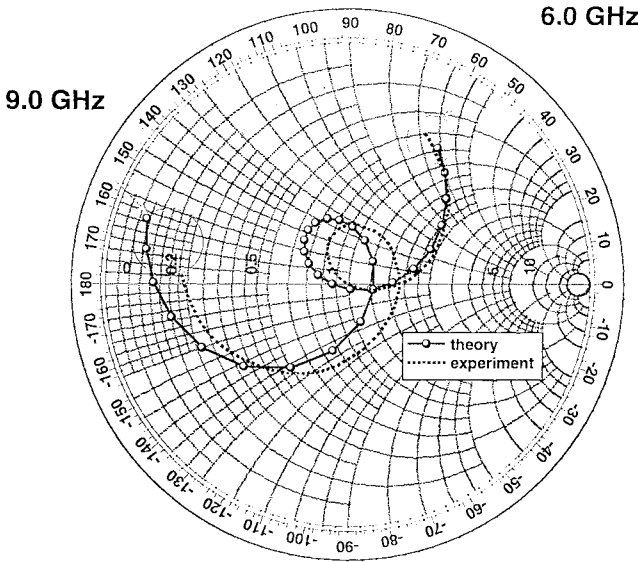


Fig. 2. Predicted and measured input impedance of probe-fed rectangular stacked-patch (parameters:  $\epsilon_{r1} = 2.2$ ,  $d_1 = 1.524$  mm,  $\tan \delta_1 = 0.001$ ,  $\epsilon_{r2} = 1.07$ ,  $d_2 = 2.5$  mm,  $\tan \delta_2 = 0.001$ ,  $L_1 = 13.5$  mm,  $W_1 = 12.5$  mm,  $L_2 = 15.0$  mm,  $W_2 = 16.0$  mm,  $x_p = 5.4$  mm,  $r_0 = 0.325$  mm).

computational time of each formulation varied according to the inherent symmetries of the configurations.

To validate the incorporated analyzes, a broad-band probe-fed stacked rectangular patch antenna was designed and developed. Fig. 2 shows the predicted and measured impedance behavior of the antenna (refer to the figure caption for the relevant dimensions). For the analysis, one attachment mode and 18 entire domain basis functions were used (nine per patch). As can be seen from Fig. 2, very good agreement between experiment and theory was achieved. The predicted and measured 10-dB return-loss bandwidths of the antenna were 27% and 26%, respectively. The bandwidth presented here is considerably larger than previous probe-fed patch configurations. Validations for the stacked circular and annular ring codes can be founded in [7] and [9] and so for the sake of brevity will not be repeated here.

### III. DESIGN TRENDS

As mentioned previously, the main purpose of this work is to develop a design strategy for probe-fed stacked-patch antennas. It should be pointed out that the trends derived here could be applied to edge-fed configurations due to the similarity of these feeding techniques as well as cavity backed configurations (for example [10]).

#### A. Substrates

A lot of research over the years has focused on what are the best materials for the dielectric layers for microstrip patches. It has been shown that thick low dielectric constant laminates tend to give the largest bandwidth responses and good surface wave efficiencies [1], [3]. Although it should be stated a combination of high dielectric constant and low dielectric constant materials can also yield good impedance behavior [11]. Perhaps the best choice of materials is a combination of low dielectric constant material (say  $\epsilon_r = 2.2$ ) and foam. This tends to give the largest impedance bandwidth and also has the simplest design procedure. Using two layers of foam does give better surface wave efficiency, however, at the expense of bandwidth reduction [3]. We have found that using the higher dielectric constant laminate for the substrate of the lower patch gives enhanced results. This can be attributed to the coupling of the modes on each patch. Unlike in [3] where the “mutual coupling” terms are the important factors in the design, here the resulting bandwidth is predominantly governed by the current distribution on the lower patch. The broadest bandwidths were achieved when the first-order mode on the lower patch is considerably greater in magnitude than the corresponding mode on the top patch. In other words, the top patch is “loosely coupled.” To do so requires the lower dielectric layer to have a greater dielectric constant than the upper layer. If the layers have the same dielectric constant or the upper layer has a higher value, the modes are too strongly coupled yielding very tight resonant loops and resulting in lower impedance bandwidths.

The thickness of each layer in a direct contact stacked-patch configuration plays an important role in the overall achievable bandwidth. Consider the lower dielectric layer  $d_1$  in Fig. 1. Obviously, the thicker the lower layer, the greater the bandwidth, however, here is where the first tradeoff must be made. The lower patch must be overcoupled to achieve a good impedance response. Thus, rather than the lower patch being designed for minimum return loss in the desired band, the patch should be strongly capacitive over this frequency range. An obvious way of doing so is to position the feed near one of the radiating edges and operate the patch above resonance, however, this has limited success. An important trend is as follows: the thicker the substrate, the less capacitive the impedance of the patch can become [1]. Thus, if the lower substrate is too thick, when the parasitically coupled patch is positioned onto the configuration, the overall impedance trend will appear inductive and the impedance control and, hence, achievable bandwidth will be limited. This effect is shown in Fig. 3 for two stacked circular patch configurations. The first Smith Chart shows the impedance loci for a single-layered patch and the effect of locating the parasitically coupled element. The presence of the second element moves the very capacitive impedance region of the single patch locus to near a matched condition. The bandwidth of this stacked-patch configuration is 28%. The second Smith Chart shows the case where an electrically thicker dielectric layer is used below the lower patch and the resulting effect on the impedance locus of the stacked configuration. Note the impedance after the first

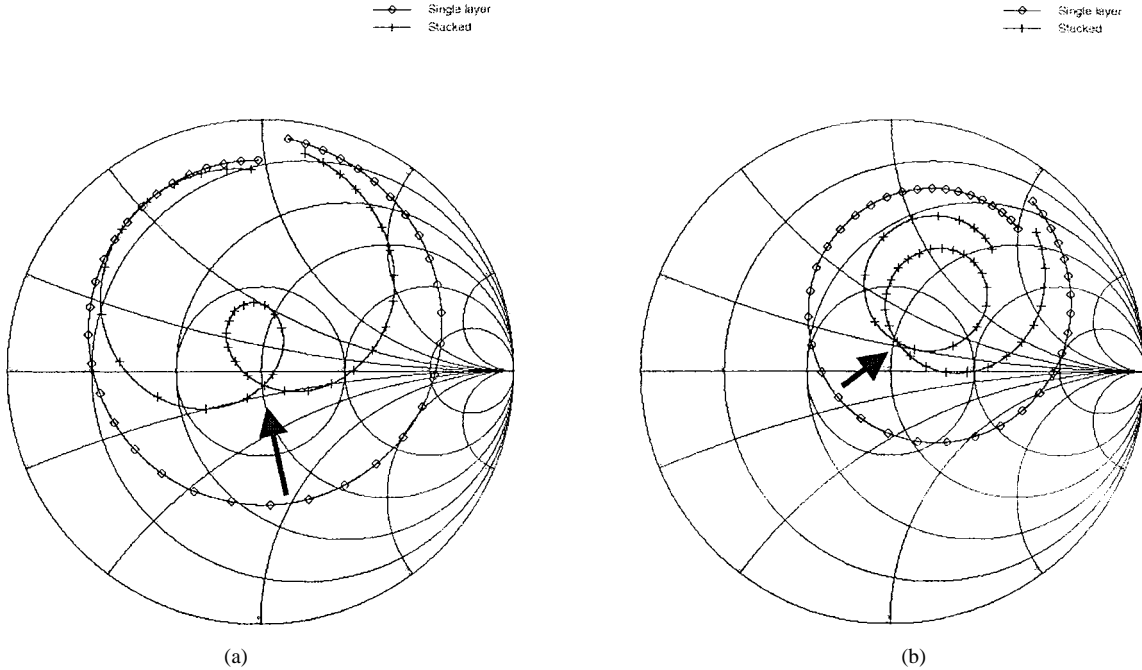


Fig. 3. Effect of  $d_1$  on stacked-patch design (frequency range: 6–11 GHz). (a) Parameters:  $\epsilon_{r1} = 2.2$ ,  $d_1 = 1.524$  mm,  $\tan \delta_1 = 0.001$ ,  $\epsilon_{r2} = 1.07$ ,  $d_2 = 2.5$  mm,  $\tan \delta_2 = 0.001$ ,  $R_1 = 7.0$  mm,  $R_2 = 7.4$  mm,  $x_p = 5.4$  mm,  $r_0 = 0.325$  mm. (b) Parameters:  $\epsilon_{r1} = 2.2$ ,  $d_1 = 2.524$  mm,  $\tan \delta_1 = 0.001$ ,  $\epsilon_{r2} = 1.07$ ,  $d_2 = 2.5$  mm,  $\tan \delta_2 = 0.001$ ,  $R_1 = 7.0$  mm,  $R_2 = 7.6$  mm,  $x_p = 5.5$  mm,  $r_0 = 0.325$  mm).

resonance of the second single layer example is considerably less capacitive than the first one. To achieve flexible impedance control of the antenna a thin layer is required for the lower material. Thus, there is a compromise between impedance control and achievable bandwidth.

Consider now the thickness of the second layer  $d_2$ .  $d_2$  essentially controls the tightness of the resonant loop or the interaction between the two patches: the further the second patch is away from the lower patch, the tighter the loop. Thus, if a lower return-loss limit is required (for example a 15-dB return-loss bandwidth), the thickness of  $d_2$  should be increased. Of course, this comes at the expense of a reduced frequency range of operation. The height of  $d_2$  is very much dependent on that of  $d_1$ : the greater  $d_1$ , the less freedom available for the selection of  $d_2$ . Typically, if  $d_1$  is too electrically thick (for example the value used in the second Smith Chart in Fig. 3),  $d_2$  must be electrically thick as well and, therefore, the overall bandwidth is not improved.

### B. Starting Point

We have found through numerous simulations that to achieve maximum bandwidths,  $d_1$  should be approximately  $0.04\lambda_0$  and  $d_2$  should be approximately  $0.06\lambda_0$ . These values were obtained using the combination of the dielectric layers suggested previously.

The dimension of the patches is obviously dependent on the geometry of conductors used, however, a reasonable starting point is to make the outer dimensions (length of the rectangular patches, diameter of the circular patches, or outer diameter of the annular rings) of both conductors approximately  $\lambda_g/2$  where  $\lambda_g$  is a guided wavelength in the lower dielectric

material. Any of the typically used approximations for a single-layered patch [12] could also be utilized, however, at this stage in the design, it is not that critical. As mentioned previously, the lower patch must be overcoupled so the feed should be positioned for an input impedance of approximately  $250\Omega$  at resonance (note: this is without the upper patch present). This resonance should be at a frequency slightly less than the lower edge of the desired band. Importantly, the impedance should have a negative reactance in the required bandwidth, with the locus outside the VSWR 2.5:1 circle. Doing so will ensure that when the top patch is positioned, the overall impedance behavior will not be too inductive. Once these steps have been carried out a resonant loop for the stacked configuration should appear in the input impedance response of the antenna. Unfortunately, it will not typically be located around the centre of the Smith Chart. The next subsection will outline how the loop can be shifted to a better location.

### C. Patch Conductor Dimensions

Once the resonant loop has been formed, adjusting the dimensions of the patches can control its location on the Smith Chart. In this section, only circular patches are presented, however, the same trends are achieved when varying the patch conductor sizes of rectangular patches ( $L_1, L_2$ ) and annular rings ( $b_1, b_2$ ). Fig. 4(a) shows the effect of varying  $R_1$  on the impedance locus while keeping the other parameters of the stacked patch constant. Note that an arc can be drawn through the centre of the resonant loops and the position of the local minimum of this arc is dependent on the thickness of  $d_1$ . As  $R_1$  is decreased the center of the resonant loop shifts from a high real component to a lower impedance. Fig. 4(b) shows the

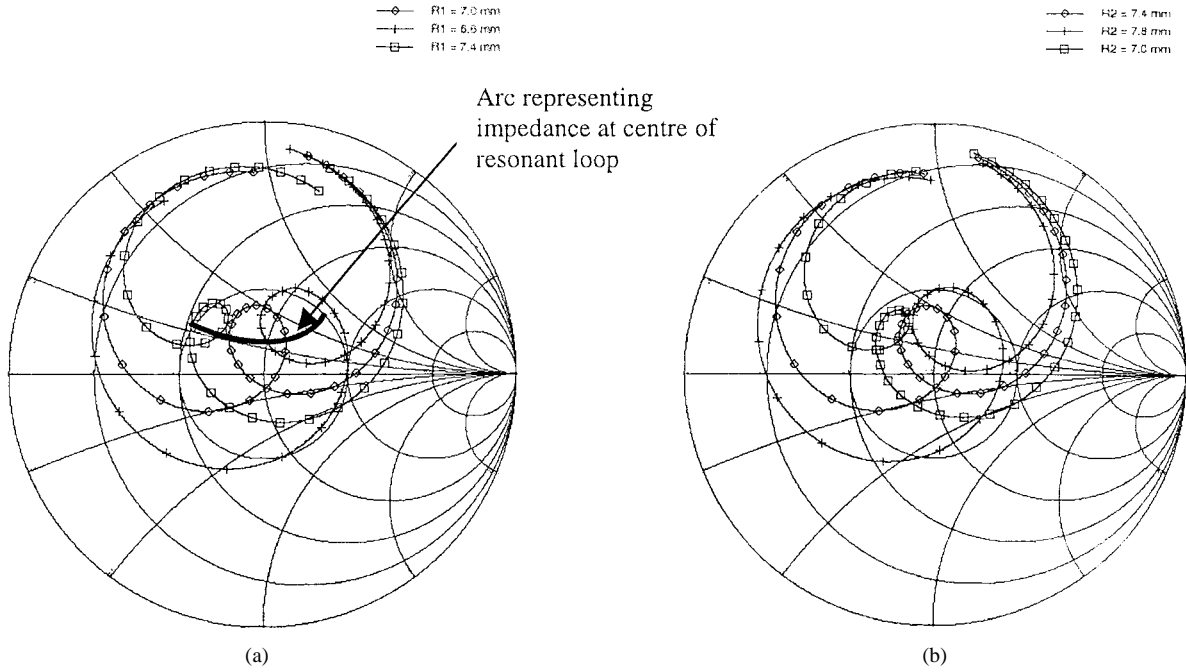


Fig. 4. Effects of patch dimensions on impedance locus (frequency range: 6–11 GHz). Parameters:  $\epsilon_{r1} = 2.2$ ,  $d_1 = 1.524$  mm,  $\tan \delta_1 = 0.001$ ,  $\epsilon_{r2} = 1.07$ ,  $d_2 = 2.5$  mm,  $\tan \delta_2 = 0.001$ ,  $x_p = 5.4$  mm,  $r_0 = 0.325$  mm. (a)  $R_1$  variation ( $R_2 = 7.4$  mm). (b)  $R_2$  variation ( $R_1 = 7.0$  mm).

effect of varying  $R_2$  on the impedance behavior of the stacked patch configuration, once again keeping all other parameters constant. Here increasing  $R_2$  increases the real component of the input impedance. Thus, changing  $R_1$  and  $R_2$  have contrary effects on the overall behavior. This is very important when designing the stacked configuration for a particular frequency band. For example, if the resonant loop occurs at the desired frequency band, however, the real part of the impedance at the center of the resonant loop is low, then  $R_2$  can be increased and  $R_1$  decreased proportionally to shift the locus without affecting the desired bandwidth. Similar loci to that shown in Fig. 4 have been achieved for square and annular ring patches when varying the outer dimensions and so, for the sake of brevity, these will not be presented here.

Adjusting the probe position has only a second-order effect on the overall impedance behavior of the stacked configuration. A trend similar to that shown in Fig. 4(b) can be achieved when increasing  $x_p$ , however, the relative movement in the center of the resonant loop is by no means as extreme. Thus, changing the position of the probe really only provides a fine tuning mechanism.

#### D. Advantages of Rectangular and Annular Ring Patches

Rectangular patches and annular rings do have an extra degree of freedom in their geometries compared to circular patches. These equate to better impedance control in the design of broad-band stacked patches. The inductive nature of the impedance locus experienced when a thick lower dielectric layer is used can be countered by decreasing the width of the lower rectangular patch. This is equivalent to making the impedance of the single layered patch more capacitive and thereby giving enhanced impedance control, similar (although to a lesser degree) to using a thinner dielectric layer as stated

TABLE I  
OPTIMUM MATERIAL SELECTION

Parameter	Lower layer	Upper Layer
Dielectric Constant ( $\epsilon_r$ )	$\approx 2.2$	$\approx 1.07$
Thickness	$\approx 0.04 \lambda_0$	$\approx 0.06 \lambda_0$

in Section III-A. The enhanced control can also be achieved in an annular ring configuration by increasing  $a_1$ , the inner radius of the lower patch. However, as mentioned before, the price for achieving better impedance control is reduced bandwidth, here typically by a few percent. Simplistically, this can be related to the size of the antenna. If we reduce the volume of an antenna, for example, by reducing the width of a patch the bandwidth will decrease. This is indeed the case for the rectangular patches where the width is reduced and for the annular rings where the inner radius is increased. Varying the width of the top rectangular patch and the inner radius of the annular ring has minor effects on the impedance loci of these stacked patches.

#### IV. CONCLUSIONS

In this paper, we have presented a procedure on how to design probe-fed stacked patches with bandwidths in excess of 25%. To achieve this degree of bandwidth a combination of low dielectric constant material and foam for the lower and upper dielectric layers, respectively, should be used. We have also discussed how the parameters effect the impedance locus of the stacked configuration and which parameters should be varied to obtain the desired response. The procedure outlined is also applicable to edge-fed stacked configurations and cavity backed patches. Summaries of the optimum material and the effects of each parameter on the impedance behavior of the stacked configuration are given in Tables I and II.

TABLE II  
EFFECTS OF PARAMETER VARIATION ON INPUT IMPEDANCE LOCUS

Parameter	$Z_{in}$ of Resonant Loop	Overall Effect
$R_1$ (or $L_1, b_1$ ) $\uparrow$	$\uparrow$ real part	Significant change in locus
$R_2$ (or $L_2, b_2$ ) $\uparrow$	$\downarrow$ real part	Significant change in locus
$x_p \uparrow$	$\uparrow$ real part	Minor change in locus
$W_1 \downarrow$ or $a_1 \uparrow$	Less inductive	$\downarrow$ bandwidth
$W_2 \downarrow$ or $a_2 \uparrow$	Minor effect	Very minor change

#### ACKNOWLEDGMENT

The author would like to thank R. Green and D. Welch for the fabrication of the stacked-patched antenna and Dr. D. Kokotoff for use of his Smith Chart plotting code.

#### REFERENCES

- [1] D. M. Pozar and D. H. Schaubert, *Microstrip Antenna Design*. Piscataway, NJ: IEEE Press, 1995.
- [2] P. S. Hall, "Probe compensation in thick microstrip patches," *Electron. Lett.*, vol. 23, pp. 606-607, 1987.
- [3] S. D. Targonski, R. B. Waterhouse, and D. M. Pozar, "Design of wide-band aperture-stacked patch microstrip antennas," *IEEE Trans. Antennas Propagat.*, vol. 46, pp. 1245-1251, Sept. 1998.
- [4] J. T. Aberle and D. M. Pozar, "Accurate and versatile solutions for probe fed microstrip patch antennas and arrays," *Electromagn.*, vol. 11, pp. 1-19, Jan. 1991.
- [5] A. N. Tulintseff, S. M. Ali, and J. A. Kong, "Input impedance of a probe-fed stacked circular microstrip antenna," *IEEE Trans. Antennas Propagat.*, vol. 39, pp. 381-390, Mar. 1991.
- [6] R. C. Hall and J. R. Mosig, "The analysis of coaxially fed microstrip antennas with electrically thick substrates," *Electromagn.*, vol. 9, pp. 367-384, Oct. 1992.
- [7] R. B. Waterhouse, M. Lye, and S. D. Targonski, "Design of printed antennas for mobile base station applications," in *3rd Asia-Pacific Conf. Commun. APCC'97*, Sydney, Australia, Dec. 1997, pp. 242-246.
- [8] J. T. Aberle, D. M. Pozar, and J. Manges, "Phased arrays of probe-fed stacked microstrip patches," *IEEE Trans. Antennas Propagat.*, vol. 42, pp. 920-927, July 1994.
- [9] D. M. Kokotoff, J. T. Aberle, and R. B. Waterhouse, "Rigorous analysis of probe-fed printed annular rings," *IEEE Trans. Antennas Propagat.*, vol. 47, pp. 384-388, Feb. 1999.
- [10] F. Zavosh and J. T. Aberle, "Infinite phased arrays of cavity-backed patches," *IEEE Trans. Antennas Propagat.*, vol. 42, pp. 390-398, Mar. 1994.
- [11] W. Rowe, R. B. Waterhouse, A. Nirmalathas, and D. Novak, "Integrated antenna base station design for hybrid fiber radio networks," in *IEEE Int. Topical Meet. Microwave Photon.*, Melbourne, Australia, Nov. 1999, pp. 47-50.
- [12] C. A. Balanis, *Antenna Theory: Analysis and Design*. New York: Wiley, 1997.

**Rod B. Waterhouse** (S'89-M'94), for a biography, see this issue, p. 1771.